Proceedings of the Pakistan Academy of Sciences: A Physical and Computational Sciences 62(1): 21-30 (2025)

ISSN (Print): 2518-4245; ISSN (Online): 2518-4253
http://doi.org/10.53560/PPASA(62-1)874

Pakistan Academy of Sciences

Research Article

Entropy Generation Analysis for the Peristaltic Motion of Ree-Eyring Fluid through a Porous Symmetric Channel under Slip Constraints

Zaheer Abbas, Muhammad Yousuf Rafiq, Salita Yaqoob, and Hafiz Shahzad*

Department of Mathematics, the Islamia University of Bahawalpur, 63100, Bahawalpur, Pakistan

Abstract: Peristaltic-driven flows play a critical role in many natural biological processes and have inspired numerous applications in engineering, medicine, and environmental technology. By mimicking the efficient movement and control of peristaltic, scientists and engineers can develop innovative solutions for a wide range of challenges. Therefore, this article delves into the peristaltic flow of electrically conducting Ree-Eyring fluid in a non-uniform symmetric conduit with entropy generation. Slip constraints and radiative impacts are also deliberated. The lubrication theory hypothesis is utilized to compress the normalized equations. Closed-form outcomes are derived and exhibited graphically to depict the distributions of velocity, entropy generation, temperature, and pressure optimization. The outcomes of this investigation showed that the liquid velocity is demoted by improving the Ree-Eyring and slip parameters. Further, the liquid temperature is boosted by augmenting the values of the Ree-Eyring fluid parameter and Brinkman number.

Keywords: Peristaltic Flow, Slip Conditions, Ree-Eyring Fluid, Entropy Generation, Thermal Radiation, Exact Solution.

1. INTRODUCTION

Peristalsis insinuates the synchronized, periodic contraction and relaxation of muscles responsible for propelling constituents through tubular organs like the esophagus, stomach, intestines, or various segments of the digestive system. This elaboration is essential for moving food, liquids, and other substances throughout the gastrointestinal tract. Within the digestive system, peristalsis aids in transporting ingested material from one segment to another, thereby facilitating digestion and absorption processes. Peristalsis is a process that involves muscle contractions creating a wave-like motion to push the contents forward. It helps move swallowed food from the mouth to the stomach in the esophagus. This process occurs mechanically and involuntarily, without conscious effort. The autonomic nervous system plays a crucial role in regulating peristalsis to ensure that it happens in a coordinated and efficient manner. The mechanical properties of peristalsis were first studied by Latham [1]. The movement of fluids by a peristaltic pump was examined in this work. In a non-uniform conduit, Vaidya *et al.* [2] discovered the stimulus of viscosity and heat conductivity fluctuations on the peristaltic behavior of Rabinowitsch liquid while considering convective surface conditions and wall characteristics. The peristaltic passage has been extensively studied, with several studies examining hypothetical and applied features. In the entropy generation study, Akbar and Abbasi [3] observed at the consequences of mixed convection, thermophoresis, variable viscosity, Brownian motion, and peristaltic-driven nanofluid movement in an asymmetric channel. The diffusion impacts on the blood flow of nanomaterials in an asymmetric conduit with the lubrication hypothesis were studied by Asha and Sunitha [4]. Rafiq and Abbas [5] researched into the results of heat radiation and viscous dissipation on the peristaltic flow of Rabinowitsch liquid in an unevenly sloped conduit. Through the use of a lubrication hypothesis, the influences of velocity slip and entropy production on the MHD peristaltic flow of an incompressible fluid in a diverging duct were predicted by Abbas *et*

Received: February 2024; Revised: February 2025; Accepted: March 2025
* Corresponding Author: Hafiz Shahzad <shahzad.gulzarr@gmail.com>

al. [6]. Using Rosseland's approximation, Farooq and Hussain [7] discussed the radiative blood flow of Williamson liquid over the esophagus. Priam and Nasrin [8] deliberated the thermally radiative peristaltic movement of time-dependent Casson liquid over a conduit having sinusoidal sides. Devakar *et al.* [9] provided a description of how a magnetic field affects the peristaltic activity of a non-Newtonian liquid inside an endoscope. Nadeem *et al.* [10] acquired critical effects for the flow fields by scrutinizing the sinusoidal flow of viscous liquid in an elliptic conduit. Numerous substantial studies concerning peristaltic flow in diverse geometries have been deliberated in previous studies [11-15].
Numerous models have been established to illustrate the comportment of non-Newtonian liquids due to their widespread usage in a variety of sectors, including engineering and industry. The Ree-Eyring model is one such model that is used in rheology to clarify the flow performance of non-Newtonian liquids, particularly those that include viscoelastic characteristics. This model works very well for relating the performance of biological liquids, polymer solutions, and other complicated materials where shear-thinning and viscoelasticity are important. The performance of Ree-Eyring liquids in several settings has been examined by numerous researchers. A general theory of non-Newtonian flow is established on Eyring's theory of rate progressions in Glasstone *et al.* [16]. After some time, this theory has been developed by Ree and Eyring [17]. Bou-Chakra *et al.* [18] used the Ree-Eyring theory to scrutinize the effects of the heterogeneous flow from coated layer surfaces on the frictional reaction and the structure of molecules in the interface region. In their study of the flow of Ree-Eyring liquid between two infinitely matching plates, Ramesh and Eytoo [19] took into account magnetic fields, radiation, heat transfer, slip boundary conditions, and porous materials. While velocity falls as the Hartmann number grows, their study revealed that temperature upsurges with greater Ree-Eyring liquid, temperature, radiation, and slip parameters. Consuming the Cattaneo–Christov model of heat movement, Abbas *et al.* [20] scrutinized the behavior of an electrically conducting Eyring–Powell liquid in a semipermeable bent conduit. Al-Mdallal *et al.* [21] scrutinized the Ree-Eyring liquid move between two stretchy turning disks packed with nanoparticles using water-base fluid by using the Runge-Kutta-Felberg technique. Tanveer and Malik [22] examined the impact of MHD and nanoparticles in a conduit using the Ree-Eyring model as a base fluid. In order to get mathematical formulas for velocity profiles and other pertinent factors, they used the lubrication technique. Rao *et al.* [23] examined the radiative characteristics of the dissipative bioconvective movement of Ree-Eyring NF over a sloping plate. Shah *et al.* [24] analyzed heat transmission properties, considering high thermal resistance and including viscous dissipation, using the Cattaneo-Christov model for Ree-Eyring NF surge across a widening sheet. The two-wave sinusoidal cilia beating inside a tubular conduit exhibit peristaltic rheology, as described by Turkyilmazoglu [25].

Entropy, which is widely used to describe the degree of disorder in a system, is a property of an irretrievable method in which the heat energy produced cannot be transformed into productive activity. Several variables, such as Joule heating, viscous dissipation, and sudden thermal radiation, affect this process. Bejan [26] was one of the pioneers in identifying entropy generation in heat transformation exploration. Akbar [27] observed elevated entropy summaries near a vertical duct while studying the peristaltic behavior of a suspension nanofluid containing carbon nanotubes (CNTs). Rashidi *et al.* [28] scrutinized entropy in peristaltically stimulated blood circulation under the influence of Lorentz force, disregarding inertial effects. Asha and Deepa [29] investigated the peristaltic circulation of blood, considered as a magneto-micropolar liquid, in a non-uniform conduit, focusing on the influences of heat radiation and entropy. Bibi and Xu [30] modeled the peristaltic flow of Jeffrey nanofluid in a symmetric conduit influenced by a magnetic field, demonstrating entropy control through various parameter estimations. The study addresses endoscopic and homogeneous-heterogeneous effects in the magnetohydrodynamic peristalsis of Ree-Eyring liquid by Hayat *et al.* [31]. Rajashekhar *et al.* [32] studied the peristaltic flow of a Ree–Eyring liquid over a uniform compliant duct, incorporating the impacts of variable viscosity and thermal conductivity in their modeling. Balachandra *et al.* [33] improved a model that includes variations in viscosity and thermal conductivity, which play a crucial role in scrutinizing blood moves in tapered arteries Shoaib *et al.* [34] explored the Optimization of entropy generation in the dissipative surge of a

Ree-Eyring liquid model, incorporating a quartic autocatalytic chemical reaction between two rotating disks. The study utilized an artificial neural systems model, which was back-propagated using the Bayesian Regularization procedure. Zafar *et al.* [35] recently studied entropy creation in the Darcy-Forchheimer Ree-Eyring nanoparticles with bioconvection flow over an elastic surface, providing a detailed exploration of the topic. Several key studies relevant to this investigation have been conducted previously [36-41].

This work covers the noted research gap and tackles real-world applications by the features of entropy production that occur when Ree-Eyring fluid peristaltically moves within a horizontal symmetric divergent channel while taking viscous and thermally radiative dissipation into consideration. Analyzing the risk of cardiac illnesses and studying hemodynamics need an understanding of how blood circulates via a horizontal symmetric diverging channel. Nonetheless, since the governing mathematical equations are extremely nonlinear, such investigations are intrinsically complicated. Ree-Eyring fluid peristaltically moves within a horizontal symmetric divergent channel, exhibit superior viscous and thermally radiative dissipation, rendering them extremely pertinent to applications in biomedicine. The complexity of the equations governing the movement of the Ree-Eyring fluid is reduced by utilizing the lubrication approximation. These results are especially important for designing curved geometries in medical implants and flow control devices. In light of this, the main goal of this research is to examine how Ree-Eyring fluid behaves as it peristaltically travels through a horizontally symmetric diverging channel. Approximate findings for heat transfer, pressure gradient, and velocity are obtained using the perturbation approach. To examine the changes in various stream characteristics under a range of important circumstances, graphical representations are used. This study is highly relevant to endoscopy, an essential diagnostic instrument for assessing the condition of internal organs. Additionally, understanding the variations in pressure gradients is crucial for regulating flow rates, especially during the insertion of catheters into arteries. Using 2D graphs, the impacts of important factors on temperature distribution and axial velocity are thoroughly analyzed, and Table 1 highlights the novel aspects of the problem.

2. MATHEMATICAL ANALYSIS

Consider the two-dimensional thermally radiative flow of Ree-Eyring fluid through a symmetric channel having wavy boundaries occupied by a porous medium. The generated flow is peristaltic. The mathematical expression in Equation (1) describes the vertical margins of the conduit [28].

$$H(\bar{x},\bar{t}) = \bar{a}\, sin\frac{2\pi}{\lambda}(\bar{x} - \bar{c}\bar{t}) + b(\bar{x}) \qquad (1)$$

where $b(\bar{x}) = b_0 + K_0\bar{x}$ and $K_0 \ll 1$ is constant and b_0 indicates the semi-width at the cove of the irregular conduit, b indicates semi-width as a role of axial distance $\bar{x}$, $\bar{a}$ indicates the amplitude of the peristaltic wave, λ indicates the wavelength of the peristaltic wave, and $\bar{t}$ indicates time as shown in Figure 1.

Table 1. Novel aspects of the present problem.

Ref. No.	[3]	[34]	[28]	[38]	Present
Peristaltic Flow	✓	✓	✓	✓	✓
Ree-Eyring Fluid	×	✓	✓	✓	✓
Entropy generation	✓	×	✓	✓	✓
Thermal radiation	×	×	×	×	✓
Slip Conditions	×	✓	×	×	✓
Porosity	×	×	×	×	✓

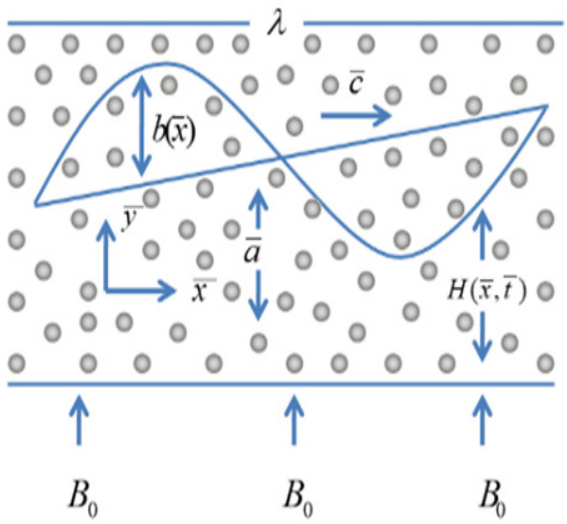

Fig. 1. Horizontal wavy porous channel.

The following Equations define the physical description of the current problems [28, 34, 38]:

$$\frac{\partial \bar{v}}{\partial \bar{y}} + \frac{\partial \bar{u}}{\partial \bar{x}} = 0 \tag{2}$$

$$\rho\left[\frac{\partial \bar{u}}{\partial \bar{t}} + \bar{v}\frac{\partial \bar{u}}{\partial \bar{y}} + \bar{u}\frac{\partial \bar{u}}{\partial \bar{x}}\right] = -\frac{\partial \bar{p}}{\partial \bar{x}} + \frac{\partial}{\partial \bar{x}}\tau_{\bar{x}\bar{x}} + \frac{\partial}{\partial \bar{y}}\tau_{\bar{x}\bar{y}} - \frac{\mu}{k}\bar{u} - \sigma B_0^2\bar{u} \tag{3}$$

$$\rho\left[\frac{\partial \bar{v}}{\partial \bar{t}} + \bar{v}\frac{\partial \bar{v}}{\partial \bar{y}} + \bar{u}\frac{\partial \bar{v}}{\partial \bar{x}}\right] = -\frac{\partial \bar{p}}{\partial \bar{y}} + \frac{\partial}{\partial \bar{x}}\tau_{\bar{y}\bar{x}} + \frac{\partial}{\partial \bar{y}}\tau_{\bar{y}\bar{y}} - \sigma B_0^2\bar{v} - \bar{v}\frac{\mu}{k} \tag{4}$$

$$C_p\left[\frac{\partial T}{\partial \bar{t}} + \bar{v}\frac{\partial T}{\partial \bar{y}} + \bar{u}\frac{\partial T}{\partial \bar{x}}\right] = \frac{k}{\rho}\left(\frac{\partial^2 T}{\partial \bar{x}^2} + \frac{\partial^2 T}{\partial \bar{y}^2}\right) - \frac{\partial q_r}{\partial y} + \frac{\tau_{\bar{x}\bar{y}}}{\rho}\left(\frac{\partial \bar{u}}{\partial \bar{y}}\right) \tag{5}$$

The stress tensor of the Ree-Eyring liquid model is:

$$\tau_{ij} = \mu\frac{\partial \bar{V}_i}{\partial \bar{x}_j} + \frac{1}{\bar{B}}sinh^{-1}\left(\frac{1}{\bar{C}}\frac{\partial \bar{V}_i}{\partial \bar{x}_j}\right) \tag{6}$$

As $\bar{sinh^{-1}}\, x = \bar{x}$ for $|\bar{x}| \leq 1$, the upstairs Equation can be rewritten as:

$$\tau_{ij} = \mu\frac{\partial \bar{V}_i}{\partial \bar{x}_j} + \frac{1}{\bar{B}}\left(\frac{1}{\bar{C}}\frac{\partial \bar{V}_i}{\partial \bar{x}_j}\right) \tag{7}$$

where, $\bar{B}$ and $\bar{C}$ represent the material coefficients and σ denotes the electrical conductivity. The dimensionless variables are:

$$x = \frac{\bar{x}}{\lambda}, \quad y = \frac{\bar{y}}{b_0}, \quad u = \frac{\bar{u}}{c}, \quad v = \frac{\bar{v}}{\delta c}, \quad t = \frac{c\bar{t}}{\lambda}, \quad \delta = \frac{b_0}{\lambda}, \quad h = \frac{H}{b_0},$$

$$p = \frac{b_0\bar{p}}{\lambda\mu c}, \phi = \frac{\bar{a}}{b_0}, \quad Re = \frac{\rho c b_0}{\mu}, \quad M = \sqrt{\frac{B_0^2 b_0^2\sigma}{\mu}}, \quad q_r = -\frac{4\sigma^*}{3k^*}\frac{\partial T^4}{\partial \tilde{y}},$$

$$\theta = \frac{T - T_0}{T_1 - T_0}, \quad Pr = \frac{\nu C_p\rho}{k}, Ec = \frac{c^2}{C_p(T_1 - T_0)}, B_r = Pr\,Ec, \quad \zeta = \frac{1}{\mu\bar{B}\,\bar{C}}$$

Where, δ stands for wave number, ϕ stands for amplitude ratio, θ stands for non-dimensional temperature, Re stands for Reynolds number, M stands for Hartmann number, q_r is the radiative heat flux, Ec stands for Eckert number, Pr represents for Prandtl number, B_r stands for Brinkmann number, and ζ stands for Ree-Eyring fluid parameter.

The dimensionless form of Equations (2), (3), (4), and (5) are:

$$Re\,\delta\left(\frac{\partial u}{\partial t} + u\frac{\partial u}{\partial x} + v\frac{\partial u}{\partial y}\right) + \frac{\partial p}{\partial x} = (1+\zeta)\left(\delta^2\frac{\partial^2 u}{\partial x^2} + \frac{\partial^2 u}{\partial y^2}\right) - M^2u - Dau\; Re\,\delta\left(\frac{\partial u}{\partial t} + u\frac{\partial u}{\partial x} + v\frac{\partial u}{\partial y}\right) + \frac{\partial p}{\partial x} = (1+\zeta)\left(\delta^2\frac{\partial^2 u}{\partial x^2} + \frac{\partial^2 u}{\partial y^2}\right) - M^2u - Dau \tag{8}$$

$$Re\,\delta^3\left(\frac{\partial v}{\partial t} + u\frac{\partial v}{\partial x} + v\frac{\partial v}{\partial y}\right) + \frac{\partial p}{\partial y} = \delta^2(1+\zeta)\left(\delta^2\frac{\partial^2 v}{\partial x^2} + \frac{\partial^2 v}{\partial y^2}\right) - \delta^2M^2v - Dau\; Re\,\delta^3\left(\frac{\partial v}{\partial t} + u\frac{\partial v}{\partial x} + v\frac{\partial v}{\partial y}\right) + \frac{\partial p}{\partial y} = \delta^2(1+\zeta)\left(\delta^2\frac{\partial^2 v}{\partial x^2} + \frac{\partial^2 v}{\partial y^2}\right) - \delta^2M^2v - Dau \tag{9}$$

$$RePr\,\delta\left(\frac{\partial\theta}{\partial t}+v\frac{\partial\theta}{\partial y}+u\frac{\partial\theta}{\partial x}\right)=\left(\frac{\partial^2\theta}{\partial y^2}+\delta^2\frac{\partial^2\theta}{\partial x^2}\right)+Ec\,Pr(1+\zeta)\left(\frac{\partial u}{\partial y}\right)^2+Rd\frac{\partial^2\theta}{\partial y^2}RePr\,\delta\left(\frac{\partial\theta}{\partial t}+v\frac{\partial\theta}{\partial y}+u\frac{\partial\theta}{\partial x}\right)=\left(\frac{\partial^2\theta}{\partial y^2}+\delta^2\frac{\partial^2\theta}{\partial x^2}\right)+Ec\,Pr(1+\zeta)\left(\frac{\partial u}{\partial y}\right)^2+Rd\frac{\partial^2\theta}{\partial y^2} \tag{10}$$

Per lubrication theory, Equations (8-10) can be reformulated as:

$$\frac{\partial p}{\partial x}=(1+\zeta)\frac{\partial^2 u}{\partial y^2}-M^2u-\frac{1}{Da}u \tag{11}$$

$$\frac{\partial p}{\partial y}=0 \tag{12}$$

$$\frac{\partial^2\theta}{\partial y^2}=-B_r(1+\zeta)\left(\frac{\partial u}{\partial y}\right)^2-Rd\frac{\partial^2\theta}{\partial y^2} \tag{13}$$

The boundary constraints can be described as:

$$\frac{\partial u}{\partial y}=0,\theta=0,aty=0 \tag{14}$$

$$\beta(1+\zeta)\frac{\partial u}{\partial y}+u=0,\theta=1,aty=h \tag{15}$$

2.1. Entropy Generation

The entropy generation can be described as:

$$s^m_{Gen}=\frac{\kappa}{T_0^2}\left(\frac{\partial T}{\partial\tilde{y}}\right)^2+\frac{1}{T_0}\left(\mu\tau_{\tilde{x}\tilde{y}}\left(\frac{\partial\tilde{u}}{\partial\tilde{y}}\right)+\sigma B_0^2\tilde{u}^2\right) \tag{16}$$

The Equation (16) defines entropy generation through four terms, accounting for thermal heat transfer irreversibility, the magnetic field and viscous dissipation. In its dimensionless form, Equation (16) expresses the ratio of volumetric entropy generation, s^m_{Gen}, to the characteristic entropy generation, s^m_G.
In the Equation (16), entropy generation is defined using four terms, accounting for thermal heat transfer irreversibility, the magnetic field and viscous dissipation. The dimensionless form of Equation (16) are:

$$N_s=\frac{s'''_{Gen}}{s_G}=(1+R)\left(\frac{\partial\theta}{\partial y}\right)^2+\Lambda B_r(1+\zeta)\left(\frac{\partial u}{\partial y}\right)^2+\Lambda B_r M^2u^2 \tag{17}$$

2.2. Solution Procedure

The result of Equations (13) and (14) with boundary conditions of Equation (15), we have [15, 25]:

$$u=\frac{1}{M^2}\frac{dp}{dx}\left[-1+Cosh\left(\frac{My}{\sqrt{1+\zeta}}\right)Sech\left(\frac{hM}{\sqrt{1+\zeta}}\right)\right] \tag{18}$$

$$\theta=\frac{1}{8hM^4}\left[\begin{matrix}4M^4y-B_rP\frac{dp^2}{dx}(-1+2hM^2y-\zeta)(h-y)+y\left(4M^4+B_r\frac{dp^2}{dx}(1+\zeta)\right)\\ Cosh\left(\frac{2hM}{\sqrt{1+\zeta}}\right)-B_rh\frac{dp^2}{dx}(1+\zeta)Cosh\left(\frac{2My}{\sqrt{1+\zeta}}\right)\left\{Sech\left(\frac{hM}{\sqrt{1+\zeta}}\right)^2\right\}\end{matrix}\right] \tag{19}$$

The pressure gradient term obtained through instantaneous mean flow rate which is characterized as:

$$Q=-\frac{1}{M^3}hM\frac{dp}{dx}+\frac{dp}{dx}\sqrt{1+\zeta}\,Tanh\left(\frac{hM}{\sqrt{1+\zeta}}\right) \tag{20}$$

$$\frac{dp}{dx}=-\frac{M^3Q}{hM-\sqrt{1+\zeta}\,Tanh\left(\frac{hM}{\sqrt{1+\zeta}}\right)} \tag{21}$$

3. RESULTS AND DISCUSSION

This section provides a graphical analysis of the impact of various parameters on pressure, velocity, heat transfer, and entropy generation. The solution and graphics of the system can be found by consuming the DSolve command in Mathematica. A valuable approach to verifying the validity of the current findings is to conduct a comparative analysis with the previous study [38]. The accuracy and reliability of the present results, as illustrated in the graphs, are validated by the strong agreement between this study's findings and existing literature. Figure 2(a) shows how the velocity distribution is affected by the magnetic field parameter "*M*", depicting a reduction in the central region while increasing near the boundaries. Figure 2(b) illustrates the impact of the Ree-Eyring fluid parameter "ζ" on velocity, potentially emphasizing non-Newtonian characteristics. Figure 2(c) demonstrates how the porous medium parameter "*S*" affects the flow, highlighting resistance due to the porous structure. Figure 2(d) elucidates the effect of the slip parameter "β", showcasing variations in boundary behavior and improved flow due to slip conditions.

Figure 3(a) depicts the variation of pressure with wavelength "ΔP_λ", showing an overall increase in pressure as "ΔP_λ" rises. Figure 3(b) examine the influence of the Ree-Eyring liquid parameter "ζ" on pressure, illustrating a noticeable increase in pressure with higher "ζ" values due to non-Newtonian effects. Figure 3(c) explore the role of the porous medium parameter "*s*", revealing that increasing "*S*" leads to a reduction in pressure, indicating higher resistance to flow. Figure 3(d) investigate the impact of the slip parameter "*β*" and the Hartmann number "*M*" on pressure, highlighting a decrease in pressure for increasing "*β*", while a higher "*M*" results in increased pressure due to electromagnetic effects. The results of the present study are in good agreement with the results available in a previous study [21].

Figure 4(a) illustrates the upshot of the magnetic field parameter "*M*" on the temperature distribution, showing variations in heat distribution due to electromagnetic forces. Figure 4(b) shows the effect of the Ree-Eyring liquid parameter "ζ" on the temperature, identifying its role in thermal diffusion. Figure 4(c) explains the behavior of the temperature profile concerning the radiation parameter "*R*", highlighting its impact on heat transfer mechanisms. Figure 4(d) demonstrates how the Brinkman number "*Br*" affects temperature variation, emphasizing its significance in convective heat transfer. Thus, we come to know that an increment in the "*Br*" raises the heat augment in the system. A similar behavior is observed by Rafiq *et al.* [5].

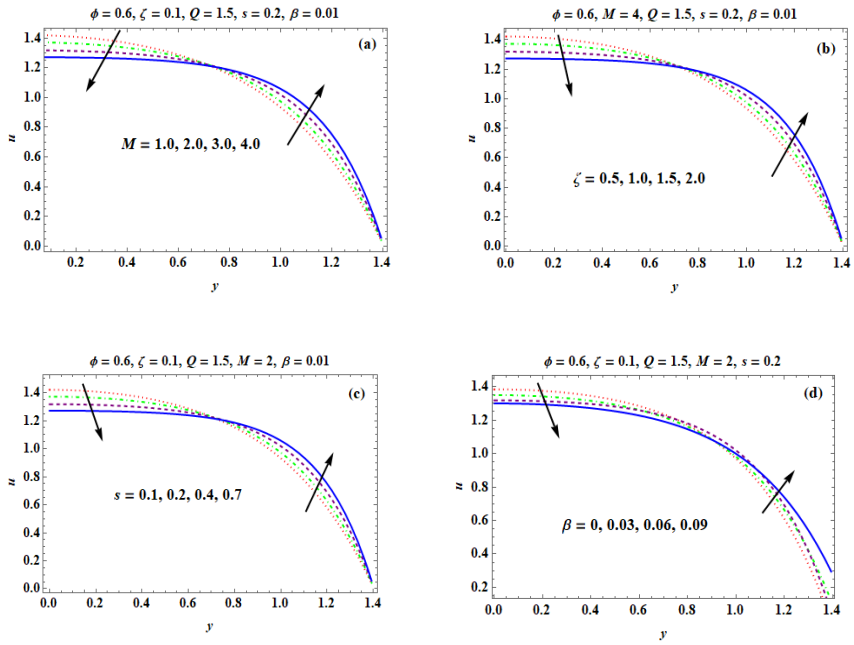

Fig. 2. Alteration of u for variation of *M* (a), ζ (b), *s* (c), and β (d).

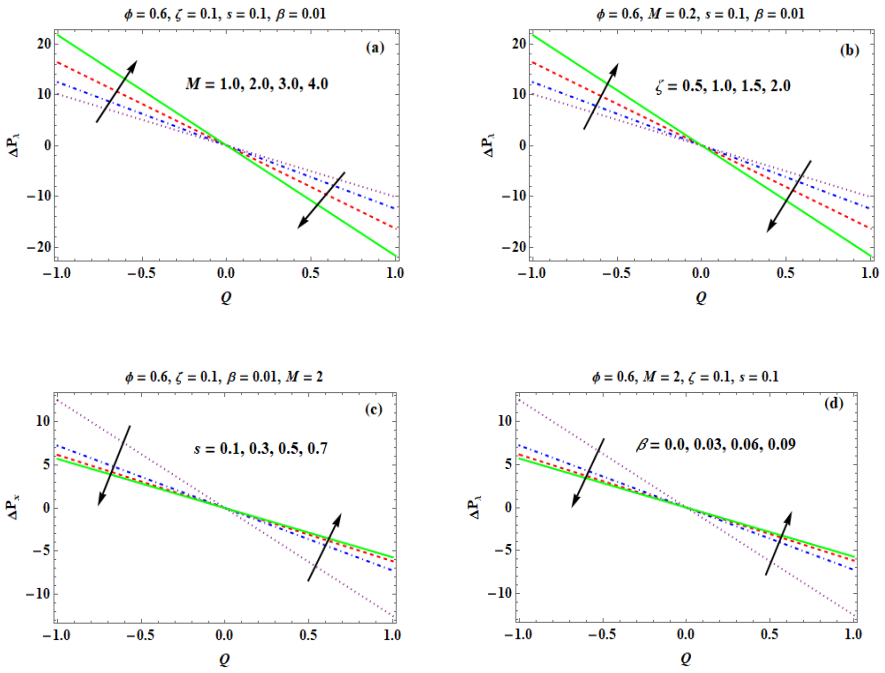

Fig. 3. Alteration of ΔP_λ for variation of M (a), ζ (b), s (c), and β (d).

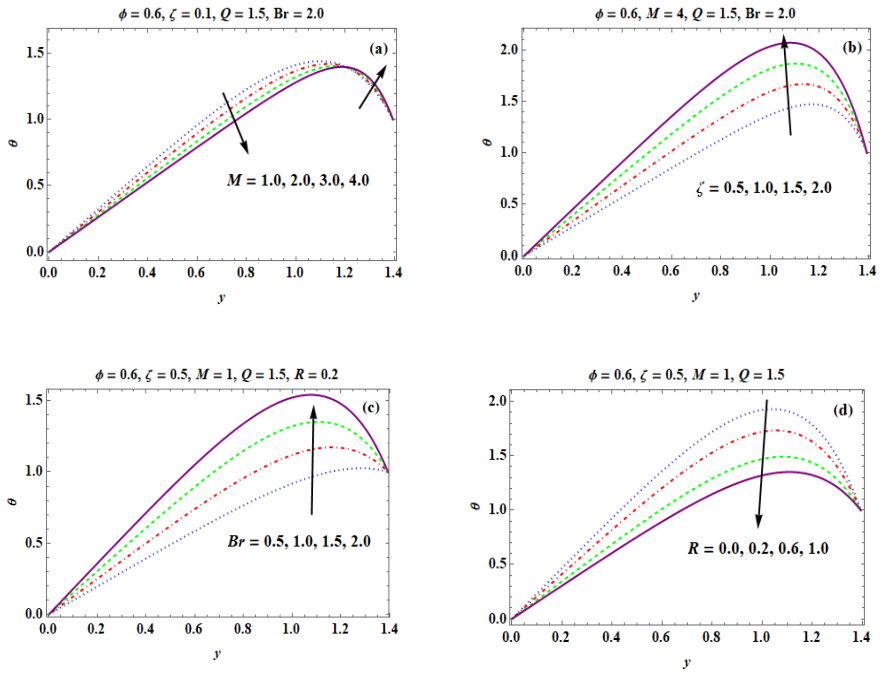

Fig. 4. Alteration of θ for variation of M (a), ζ (b), Br (c), and R (d).

Figure 5(a) demonstrates how the entropy generation changes with variations in the Ree-Eyring parameter "ζ". A decreasing trend is observed, indicating that increasing "ζ" reduces entropy production in the system. Figure 5(b) elucidates the outcome of the Brinkman number "*Br*" on entropy generation. The results reveal a continuous decline, suggesting that increasing viscous dissipation reduces entropy generation. Figure 5(c) shows the impact of the Hartmann number "*M*". As M increases, entropy generation also rises, which aligns with findings by Shoaib *et al.* [35], indicating that the presence of a stronger magnetic field improves irreversibility. Figure 5(d) displays the upshot of the wave number "*δ*" on entropy generation. A continuous upsurge in

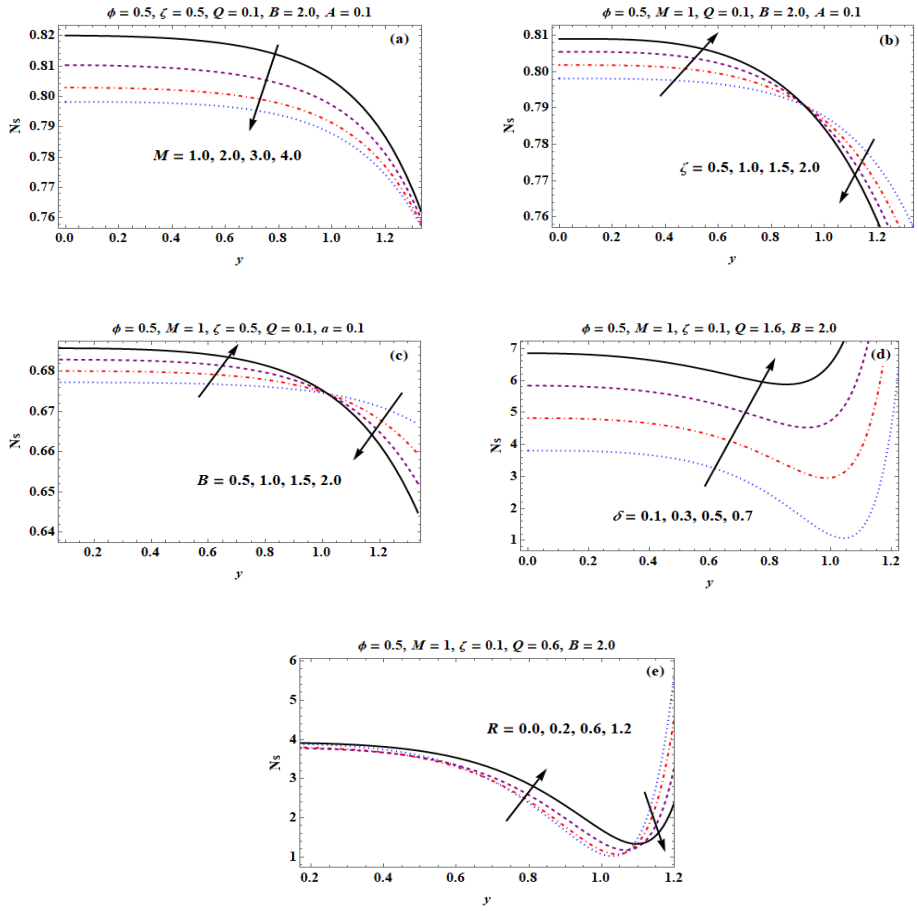

Fig. 5. Alteration of Ns for variation of M (a), ζ (b), Br (c), δ (d), and R (e).

entropy generation is observed as "δ" increases, highlighting the influence of wave characteristics on system disorder. Figure 5(e) shows the behavior of thermal radiation "R". Initially, entropy generation increases, but after reaching a threshold value (~1.1), it starts to decline. This non-monotonic trend suggests that thermal radiation has a complex effect on entropy generation.

4. CONCLUSIONS

This research investigates the behavior of Ree-Eyring liquid within a permeable medium in a symmetric tapered conduit, emphasizing the influence of thermal boundary conditions on the temperature profile and entropy generation. This study enhances our understanding of fluid flow behavior in a symmetric tapered conduit, paving the way for optimizing flow dynamics and reducing resistance. Future research can expand on this work by incorporating additional models such as the Ree-Eyring fluid model and the Oldroyd-B fluid model, along with factors like mixed convection and bioconvection. The analysis reveals that fluid velocity diminishes as the Ree-Eyring and slip parameters increase. Additionally, pressure variations show that the Ree-Eyring parameter and Hartmann number lead to a rise in the retrograde region, while a contrasting trend is observed in the co-pumping region. The Brinkman number significantly influences the system, as its increase results in greater heat inflow, elevating the liquid temperature. The temperature is also shown to rise with growing values of both the Brinkman number and thermal radiation. Furthermore, entropy generation is particularly pronounced near the channel boundaries, intensifying with higher wave number and thermal radiation values. These findings are supported by graphical representations that highlight the effects of the evolving parameters on the system.

5. ACKNOWLEDGEMENTS

We are thankful to The Islamia University of Bahawalpur for providing the research facilities to conduct this work.

6. CONFLICT OF INTEREST

The authors declare no conflict of interest.

7. REFERENCES

1. T.W. Latham. Fluid motions in a peristaltic pump. Doctoral Dissertation. *Massachusetts Institute of Technology, USA* (1966).
2. H. Vaidya, C. Rajashekhar, M. Gudekote, K.V. Prasad, O.D. Makinde, and S. Sreenadh. Peristaltic motion of non-newtonian fluid with variable liquid properties in a convectively heated nonuniform tube: Rabinowitsch fluid model. *Journal of Enhanced Heat Transfer* 26(3): 277-294 (2019).
3. Y. Akbar and F.M. Abbasi. Impact of variable viscosity on peristaltic motion with entropy generation. *International Communications in Heat and Mass Transfer* 118: 104826 (2020).
4. S.K. Asha and G. Sunitha. Thermal radiation and Hall effects on peristaltic blood flow with double diffusion in the presence of nanoparticles. *Case Studies in Thermal Engineering* 17: 100560 (2020).
5. M.Y. Rafiq and Z. Abbas. Impacts of viscous dissipation and thermal radiation on Rabinowitsch fluid model obeying peristaltic mechanism with wall properties. *Arabian Journal for Science and Engineering* 46: 12155-12163 (2021).
6. Z. Abbas, M.Y. Rafiq, A.S. Alshomrani, and M.Z. Ullah. Analysis of entropy generation on peristaltic phenomena of MHD slip flow of viscous fluid in a diverging tube. *Case Studies in Thermal Engineering* 23: 100817 (2021).
7. N. Farooq and A. Hussain. Peristaltic analysis of Williamson blood flow model with solar biomimetic pump. *International Communications in Heat and Mass Transfer* 138: 106305 (2022).
8. S.S. Priam and R. Nasrin. Numerical appraisal of time-dependent peristaltic duct flow using Casson fluid. *International Journal of Mechanical Sciences* 233: 107676 (2022).
9. M. Devakar, K. Ramesh, and K. Vajravelu. Magnetohydrodynamic effects on the peristaltic flow of couple stress fluid in an inclined tube with endoscope. *Journal of Computational Mathematics and Data Science* 2: 100025 (2022).
10. S. Nadeem, S. Akhtar, F.M. Alharbi, S. Saleem, and A. Issakhov. Analysis of heat and mass transfer on the peristaltic flow in a duct with sinusoidal walls: Exact solutions of coupled PDEs. *Alexandria Engineering Journal* 61(5): 4107-4117 (2022).
11. Z. Abbas, A. Shakeel, M.Y. Rafiq, S. Khaliq, J. Hasnain, and A. Nadeem. Rheology of peristaltic flow in couple stress fluid in an inclined tube: Heat and mass transfer analysis. *Advances in Mechanical Engineering* 14(11): 1-14 (2022).
12. S. Akhtar, S. Almutairi, and S. Nadeem. Impact of heat and mass transfer on the Peristaltic flow of non-Newtonian Casson fluid inside an elliptic conduit: Exact solutions through novel technique. *Chinese Journal of Physics* 78: 194-206 (2022).
13. N.M. Hafez, A.M. Abd-Alla, and T.M.N. Metwaly. Influences of rotation and mass and heat transfer on MHD peristaltic transport of Casson fluid through inclined plane. *Alexandria Engineering Journal* 68: 665-692 (2023).
14. J. Iqbal, F.M. Abbasi, M. Alkinidri, and H. Alahmadi. Heat and mass transfer analysis for MHD bioconvection peristaltic motion of Powell-Eyring nanofluid with variable thermal characteristics. *Case Studies in Thermal Engineering* 43: 102692 (2023).
15. M. Turkyilmazoglu. Corrections to long wavelength approximation of peristalsis viscous fluid flow within a wavy channel. *Chinese Journal of Physics* 89: 340-354 (2024).
16. S. Glasstone, K.J. Laidler, and H. Eyring (Eds.). The theory of rate processes: the kinetics of chemical reactions, viscosity, diffusion and electrochemical phenomena. *McGraw Hill, New York, USA* (1941).
17. T. Ree and H. Eyring. Theory of non-newtonian flow. I. solid plastic system. *Journal of Applied Physics* 26(7): 793-800 (1955).
18. E. Bou-Chakra, J. Cayer-Barrioz, D. Mazuyer, F. Jarnias, and A. Bouffet. A non-Newtonian model based on Ree-Eyring theory and surface effect to predict friction in elastohydrodynamic lubrication. *Tribology International* 43(9): 1674-1682 (2010).
19. K. Ramesh and S.A. Eytoo. Effects of thermal radiation and magnetohydrodynamics on Ree-Eyring fluid flows through porous medium with slip boundary conditions. *Multidiscipline Modeling in Materials and Structures* 15(2): 492-507 (2018).
20. Z. Abbas, M.Y. Rafiq, and M. Naveed. Analysis of Eyring-Powell liquid flow in curved channel with Cattaneo-Christov heat flux model. *Journal of the Brazilian Society of Mechanical Sciences and Engineering* 40(1): 390 (2018).
21. Q.M. Al-Mdallal, A. Renuka, M. Muthtamilselvan, and B. Abdalla. Ree-Eyring fluid flow of Cu-water nanofluid between infinite spinning disks with an effect of thermal radiation. *Ain Shams Engineering Journal* 12(3): 2947-2956 (2021).
22. A. Tanveer and M.Y. Malik. Slip and porosity

effects on peristalsis of MHD Ree-Eyring nanofluid in curved geometry. *Ain Shams Engineering Journal* 12(1): 955-968 (2021).
23. D.P.C. Rao, S. Thiagarajan, and V.S. Kumar. Significance of quadratic thermal radiation on the bioconvective flow of Ree-Eyring fluid through an inclined plate with viscous dissipation and chemical reaction: Non-Fourier heat flux model. *International Journal of Ambient Energy* 43(1): 6436-6448 (2022).
24. Z. Shah, N. Vrinceanu, M. Rooman, W. Deebani, and M. Shutaywi. Mathematical modelling of Ree-eyring nanofluid using Koo-kleinstreuer and Cattaneo-Christov models on chemically reactive AA 7072-AA 7075 alloys over a magnetic dipole stretching surface. *Coatings* 12(3): 391 (2022).
25. M. Turkyilmazoglu. Long wavelength analysis amendment on the cilia beating assisted peristalsis in a tube. *Theoretical and Computational Fluid Dynamics* 39(1): 3 (2025).
26. A. Bejan. A study of entropy generation in fundamental convective heat transfer. *Journal of Heat Transfer* 101(4): 718-725 (1979).
27. N.S. Akbar. Entropy generation analysis for a CNT suspension nanofluid in plumb ducts with peristalsis. *Entropy* 17(3): 1411-1424 (2015).
28. M.M. Rashidi, M.M. Bhatti, M.A. Abbas and M.E.S. Ali. Entropy generation on MHD blood flow of nanofluid due to peristaltic waves. *Entropy* 18(4): 117 (2016).
29. S.K. Asha and C.K. Deepa. Entropy generation for peristaltic blood flow of a magneto-micropolar fluid with thermal radiation in a tapered asymmetric channel. *Results in Engineering* 3: 100024 (2019).
30. A. Bibi and H. Xu. Entropy generation analysis of peristaltic flow and heat transfer of a Jeffery nanofluid in a horizontal channel under magnetic environment. *Mathematical Problems in Engineering* 2019: 2405986 (2019).
31. T. Hayat, J. Akram, A. Alsaedi, and H. Zahir. Endoscopy and homogeneous-heterogeneous reactions in MHD radiative peristaltic activity of Ree-Eyring fluid. *Results in Physics* 8: 481-488 (2018).
32. C. Rajashekhar, F. Mebarek-Oudina, H. Vaidya, K.V. Prasad, G. Manjunatha, and H. Balachandra. Mass and heat transport impact on the peristaltic flow of a Ree-Eyring liquid through variable properties for hemodynamic flow. *Heat Transfer* 50(5): 5106-5122 (2021).
33. H. Balachandra, C. Rajashekhar, F. Mebarek-Oudina, G. Manjunatha, H. Vaidya, and K.V. Prasad Slip effects on a ree-eyring liquid peristaltic flow towards an inclined channel and variable liquid properties. *Journal of Nanofluids* 10(2): 246-258 (2021).
34. M. Shoaib, G. Zubair, K.S. Nisar, M.A.Z. Raja, M.I. Khan, R.P. Gowda, and B.C. Prasannakumara. Ohmic heating effects and entropy generation for nanofluidic system of Ree-Eyring fluid: Intelligent computing paradigm. *International Communications in Heat and Mass Transfer* 129(1): 105683 (2021).
35. S.S. Zafar, A. Zaib, F. Ali, F.S. Alduais, A.A. Bossly, and A. Saeed. Second law analysis on Ree-Eyring nanoliquid and Darcy Forchheimer flow through a significant stratification in the gyrotactic microorganism. *International Journal of Numerical Methods for Heat & Fluid Flow* 34(2): 494-519 (2024).
36. M. Turkyilmazoglu. Eyring–Powell fluid flow through a circular pipe and heat transfer: full solutions. *International Journal of Numerical Methods for Heat & Fluid Flow* 30(11): 4765-4774 (2020).
37. K. Abuasbeh, B. Ahmed, A.U.K. Niazi, and M. Awadalla. Entropy generation for MHD peristaltic transport of non-Newtonian fluid in a horizontal symmetric divergent channel. *Symmetry* 15(2): 359 (2023).
38. A. Fayyaz, Z. Abbas, and M.Y. Rafiq. Analysis of Radiatively Peristaltic Flow of Ree-Eyring Fluid Through an Annulus Region Between Two Flexible Tubes with Entropy Generation. *Arabian Journal for Science and Engineering* 1-14 (2024).
39. H. Shahzad, Z. Abbas, and M.Y. Rafiq. Rheological behavior of two immiscible hybrid nanofluids with modified thermal conductivity models through a heated curved pipe. *Alexandria Engineering Journal* 122: 318-333 (2025).
40. M. Turkyilmazoglu. Slip flow between corotating disks with heat transfer. *International Journal of Numerical Methods for Heat & Fluid Flow* 35(1): 257-276 (2025).
41. A. Naeem, Z. Abbas, and M.Y. Rafiq. Study of chemical properties of hybrid nanofluid flow between two permeable disks with suspension of carbon nanotubes using Yamada Ota and Xue models. *International Journal of Thermofluids* 26: 101075 (2025).